LETTER

doi:10.1038/nature10343

Role of sulphuric acid, ammonia and galactic cosmic rays in atmospheric aerosol nucleation

Jasper Kirkby[1], Joachim Curtius[2], João Almeida[2,3], Eimear Dunne[4], Jonathan Duplissy[1,5,6], Sebastian Ehrhart[2], Alessandro Franchin[5], Stéphanie Gagné[5,6], Luisa Ickes[2], Andreas Kürten[2], Agnieszka Kupc[7], Axel Metzger[8], Francesco Riccobono[9], Linda Rondo[2], Siegfried Schobesberger[5], Georgios Tsagkogeorgas[10], Daniela Wimmer[2], Antonio Amorim[3], Federico Bianchi[9,11], Martin Breitenlechner[8], André David[1], Josef Dommen[9], Andrew Downard[12], Mikael Ehn[5], Richard C. Flagan[12], Stefan Haider[1], Armin Hansel[8], Daniel Hauser[8], Werner Jud[8], Heikki Junninen[5], Fabian Kreissl[2], Alexander Kvashin[13], Ari Laaksonen[14], Katrianne Lehtipalo[5], Jorge Lima[3], Edward R. Lovejoy[15], Vladimir Makhmutov[13], Serge Mathot[1], Jyri Mikkilä[5], Pierre Minginette[1], Sandra Mogo[3], Tuomo Nieminen[5], Antti Onnela[1], Paulo Pereira[3], Tuukka Petäjä[5], Ralf Schnitzhofer[8], John H. Seinfeld[12], Mikko Sipilä[5,6], Yuri Stozhkov[13], Frank Stratmann[10], Antonio Tomé[3], Joonas Vanhanen[5], Yrjo Viisanen[16], Aron Vrtala[7], Paul E. Wagner[7], Hansueli Walther[9], Ernest Weingartner[9], Heike Wex[10], Paul M. Winkler[7], Kenneth S. Carslaw[4], Douglas R. Worsnop[5,17], Urs Baltensperger[9] & Markku Kulmala[5]

Atmospheric aerosols exert an important influence on climate[1] through their effects on stratiform cloud albedo and lifetime[2] and the invigoration of convective storms[3]. Model calculations suggest that almost half of the global cloud condensation nuclei in the atmospheric boundary layer may originate from the nucleation of aerosols from trace condensable vapours[4], although the sensitivity of the number of cloud condensation nuclei to changes of nucleation rate may be small[5,6]. Despite extensive research, fundamental questions remain about the nucleation rate of sulphuric acid particles and the mechanisms responsible, including the roles of galactic cosmic rays and other chemical species such as ammonia[7]. Here we present the first results from the CLOUD experiment at CERN. We find that atmospherically relevant ammonia mixing ratios of 100 parts per trillion by volume, or less, increase the nucleation rate of sulphuric acid particles more than 100–1,000-fold. Time-resolved molecular measurements reveal that nucleation proceeds by a base-stabilization mechanism involving the stepwise accretion of ammonia molecules. Ions increase the nucleation rate by an additional factor of between two and more than ten at ground-level galactic-cosmic-ray intensities, provided that the nucleation rate lies below the limiting ion-pair production rate. We find that ion-induced binary nucleation of H_2SO_4–H_2O can occur in the mid-troposphere but is negligible in the boundary layer. However, even with the large enhancements in rate due to ammonia and ions, atmospheric concentrations of ammonia and sulphuric acid are insufficient to account for observed boundary-layer nucleation.

The primary vapour responsible for atmospheric nucleation is thought to be sulphuric acid. However, theory suggests that peak concentrations in the boundary layer (10^6–10^7 cm^{-3}; ref. 8) are usually too low for the binary nucleation of H_2SO_4–H_2O to proceed. Furthermore, after nucleation there is generally insufficient H_2SO_4 to grow the clusters to cloud condensation nucleus sizes (more than 50 nm), so organic species are primarily responsible for particle growth[9,10]. Nucleation of sulphuric acid particles is known to be enhanced by the presence of ternary species such as ammonia[11–13] or organic compounds[14] such as amines[15–17] or oxidized organic compounds[18,19]. Ions are also expected to enhance nucleation[20–24], and ion-induced nucleation has been observed in the atmosphere[25,26]. Because the primary source of ions in the global troposphere is galactic cosmic rays (GCRs), their role in atmospheric nucleation is of considerable interest as a possible physical mechanism for climate variability caused by the Sun[27,28].

Here we address three issues that currently limit our understanding of atmospheric nucleation and its influence on climate[7]. First, quantitative measurements of the roles of ions and ternary vapours are lacking. Second, the nucleation mechanism and the molecular composition of the critical nucleus have not been directly measured. Third, it remains an open question whether laboratory measurements are able to reproduce atmospheric observations: recent experiments have concluded that atmospheric concentrations of H_2SO_4 and H_2O without ternary vapours are sufficient[29] or insufficient[19] to explain boundary-layer nucleation rates.

We present here the first results from the CLOUD experiment at CERN (see Methods, Supplementary Information and Supplementary Fig. 1 for experimental details). The measurements, obtained at the CERN Proton Synchrotron, represent the most rigorous laboratory evaluation yet accomplished of binary, ternary and ion-induced nucleation of sulphuric acid particles under atmospheric conditions.

The nucleation rates (J, cm^{-3} s^{-1}) are measured under neutral (J_n), GCR (J_{gcr}) and charged pion beam (J_{ch}) conditions, corresponding to ion-pair concentrations of about 0, 400 and 3,000 cm^{-3}, respectively. A typical sequence of J_n, J_{gcr} and J_{ch} measurements is shown in Supplementary Fig. 2 and is described in the Supplementary Information. Both J_{gcr} and J_{ch} comprise the sum of ion-induced and neutral nucleation rates, whereas J_n measures the neutral rate alone. The nucleation rates are shown in Fig. 1 as a function of [H_2SO_4] at 248, 278 and 292 K. As the temperature is reduced, lower H_2SO_4 concentrations are sufficient to maintain the same nucleation rates, as a result of the decrease in the H_2SO_4 saturation vapour pressure. Apart from contaminants (see below), the only condensable vapours present in the chamber for these data are H_2SO_4 and H_2O. The experimental results are slightly higher than model calculations[30] based on thermochemical data for charged H_2SO_4–H_2O clusters[23] under J_{ch} ionization conditions, but they show similar curvature and slope.

The presence of ions from ground-level GCR ionization (J_{gcr} curves) enhances the neutral nucleation rate roughly twofold at 292 K and

[1]CERN, CH-1211 Geneva, Switzerland. [2]Goethe-University of Frankfurt, Institute for Atmospheric and Environmental Sciences, 60438 Frankfurt am Main, Germany. [3]SIM, University of Lisbon and University of Beira Interior, 1749-016 Lisbon, Portugal. [4]University of Leeds, School of Earth and Environment, LS2-9JT Leeds, United Kingdom. [5]University of Helsinki, Department of Physics, FI-00014 Helsinki, Finland. [6]Helsinki Institute of Physics, University of Helsinki, FI-00014 Helsinki, Finland. [7]University of Vienna, Faculty of Physics, 1090 Vienna, Austria. [8]Ionicon Analytik GmbH and University of Innsbruck, Institute for Ion and Applied Physics, 6020 Innsbruck, Austria. [9]Paul Scherrer Institut, Laboratory of Atmospheric Chemistry, CH-5232 Villigen, Switzerland. [10]Leibniz Institute for Tropospheric Research, 04318 Leipzig, Germany. [11]University of Milan, Department of Inorganic, Metallorganic, and Analytical Chemistry, 20133 Milan, Italy. [12]California Institute of Technology, Division of Chemistry and Chemical Engineering, Pasadena, California 91125, USA, [13]Lebedev Physical Institute, Solar and Cosmic Ray Research Laboratory, 119991 Moscow, Russia. [14]University of Eastern Finland, FI-70211 Kuopio, Finland. [15]NOAA Earth System Research Laboratory, Boulder, Colorado 80305, USA. [16]Finnish Meteorological Institute, FI-00101 Helsinki, Finland. [17]Aerodyne Research Inc., Billerica, Massachusetts 01821, USA.

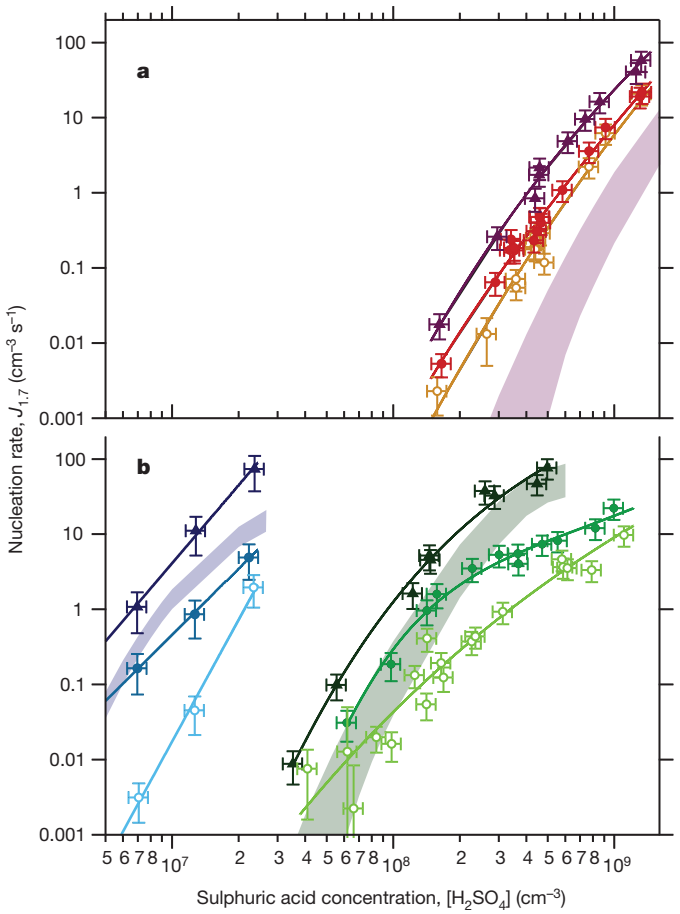

Figure 1 | Plots of nucleation rate against H_2SO_4 concentration. Neutral, GCR and charged (pion beam) nucleation rates are shown at 1.7 nm diameter, $J_{1.7}$, as a function of sulphuric acid concentration at 38% relative humidity. **a**, Rates at 292 K; **b**, rates at 248 K (blue) and 278 K (green). The NH_3 mixing ratios correspond to the contaminant level (<35 p.p.t.v. at 278 and 292 K; <50 p.p.t.v. at 248 K). Triangles, J_{ch}; filled circles, J_{gcr}; open circles, J_n. The predictions of the PARNUC model[30] for binary H_2SO_4–H_2O charged nucleation, J_{ch}, are indicated by the coloured bands. The fitted curves are drawn to guide the eye. The error bars indicate the estimated total statistical and systematic 1σ measurement uncertainties, although the overall factor 2 systematic scale uncertainty on [H_2SO_4] is not shown.

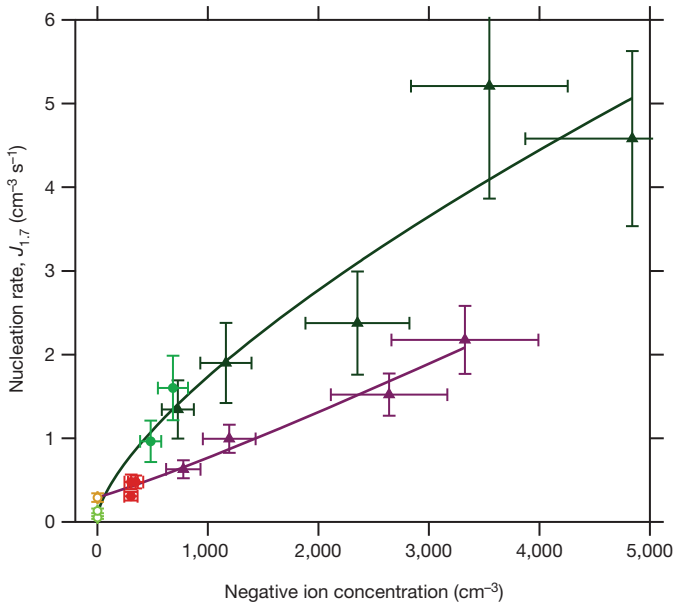

Figure 2 | Plots of nucleation rate against negative ion concentration. Nucleation rates as a function of negative ion concentration at 292 K and [H_2SO_4] = 4.5×10^8 cm^{-3} (purple line), and at 278 K and [H_2SO_4] = 1.5×10^8 cm^{-3} (green line). Triangles, J_{ch}; filled circles, J_{gcr}; open circles, J_n. All measurements were made at 38% relative humidity and 35 p.p.t.v. NH_3. Neutral nucleation rates, J_n, were effectively measured at zero ion pair concentration (ion or charged-cluster lifetime <1 s). The curves are fits of the form $J = j_0 + k[\text{ion}^-]^p$, where j_0, k and p are free parameters. The error bars indicate only the point-to-point 1σ errors; the nucleation rates and ion concentrations each have estimated overall scale uncertainties of ±30%.

more than tenfold at 278 and 248 K. The enhancement factor is up to five times larger at the higher ion-pair concentrations typical of the upper troposphere (Fig. 2, and J_{ch} curves in Fig. 1). Overall, we find that the nucleation rate varies with negative ion concentration, [ion$^-$], as $J = J_n + k[\text{ion}^-]^p$, with $p = 0.7$–1.0 (Fig. 2). Our measurements show evidence of saturation of J_{gcr} and J_{ch} by their convergence with J_n at high nucleation rates (Fig. 1), where almost every negative ion gives rise to a new particle[21]. However, even with ion enhancement, our measurements show that binary nucleation of H_2SO_4–H_2O will proceed at extremely low rates in the atmospheric boundary layer. In contrast, in the cooler mid-troposphere and perhaps at lower altitude in some polar regions, ion-induced binary nucleation can proceed at ambient acid concentrations[23].

CLOUD has measured the molecular composition of nucleating charged clusters from monomers up to stable aerosol particles, and has time-resolved each step of their growth. Example mass spectra are shown in Supplementary Fig. 3. The ion-induced nucleation measurements in Fig. 1 exclusively involve negative clusters, containing the HSO_4^-, HSO_5^- or SO_5^- ion (Supplementary Fig. 4 shows an example of a nucleation event). However, at higher ammonia concentrations (see below) we have also observed positively charged nucleation, involving the NH_4^+ ion.

The chemical composition of nucleating clusters containing up to $n = 20$ sulphuric acid molecules, including the HSO_4^- ion, is shown in Fig. 3. At 292 K the clusters above $n = 4$ are found always to be accompanied by additional nitrogen-containing molecules, comprising NH_3, amines (mainly dimethylamine and ethylamine) and urea (Fig. 3c, d). Although these ternary vapours were not intentionally added to the chamber—at least initially—they are crucial to the nucleation. The measured contaminant mixing ratios of ammonia and total amines were less than 35 parts per trillion by volume (p.p.t.v.) and less than 50 p.p.t.v., respectively. It is notable that the nucleating H_2SO_4 clusters included only nitrogen-containing bases, even though a broad spectrum of gas-phase contaminants was identified in the chamber. A clear progression is observed from almost pure binary nucleation at 248 K to pure ternary nucleation at 292 K; both binary and ternary nucleation contributed at 278 K. From the molecular measurements, the binary fraction (or upper limit) can be determined for each J_{ch} measurement. After application of these corrections, there is excellent agreement between the experimental binary J_{ch} values and the model predictions shown in Fig. 1.

Further measurements were made with NH_3 intentionally added to the chamber. The nucleation rates were highly sensitive to small additions of ammonia up to about 100 p.p.t.v., with evidence of saturation at higher mixing ratios (Fig. 4). In some cases the saturation also resulted from the ionization rate limits of about 4 cm^{-3} s^{-1} for GCRs and 80 cm^{-3} s^{-1} for the pion beam. The onset of positively charged nucleation was observed at about 900 p.p.t.v. NH_3 at 292 K and at 300 p.p.t.v. NH_3 at 278 K, which contributed to a further rise of J_{gcr} and J_{ch}. With additional NH_3 the nucleating clusters revealed a distinctive increase in the NH_3 molecular content (compare Fig. 3c with Fig. 3d). These observations provide clear experimental evidence that the nucleation rates are strongly limited by the availability of NH_3 at mixing ratios below 100 p.p.t.v., and further strengthen our argument that binary nucleation is not significant in the global boundary layer.

The negative cluster ion spectra (Fig. 3) show strong, quasi-stable peaks corresponding to the charged pure monomer, dimer and trimer

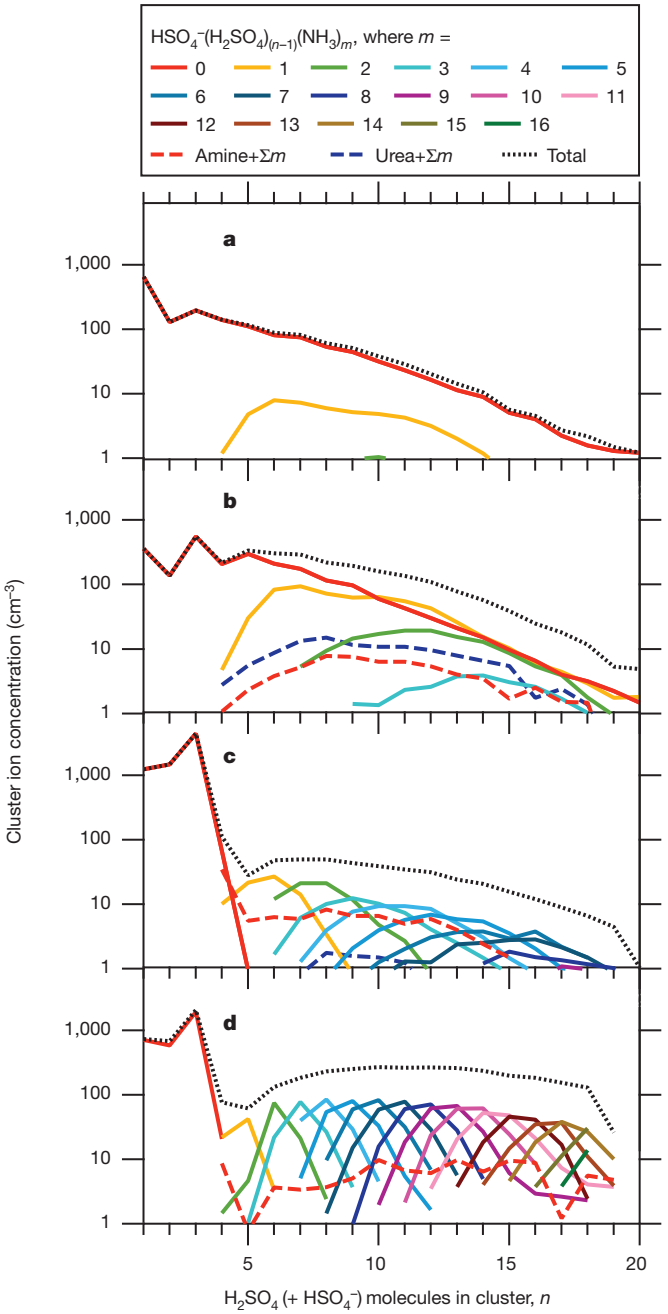

Figure 3 | Ion cluster composition. **a–d**, The chemical composition of charged nucleating clusters at 248 K (<35 p.p.t.v. NH_3) (**a**), 278 K (<35 p.p.t.v. NH_3) (**b**), 292 K (<35 p.p.t.v. NH_3) (**c**) and 292 K (230 p.p.t.v. NH_3) (**d**). The cluster spectra are averaged over the steady-state nucleation period. To simplify the figures, only the overall envelopes are shown for organic species. The concentrations are approximately corrected for detection efficiency.

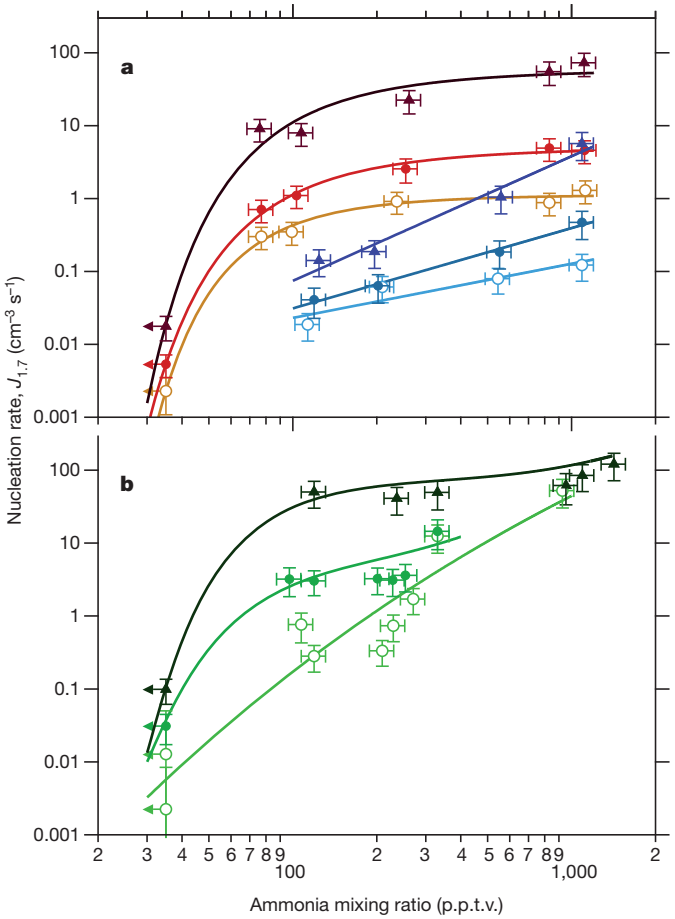

Figure 4 | Plots of nucleation rate against NH_3 concentration. Nucleation rates are shown as a function of ammonia mixing ratio. **a**, At 292 K and $[H_2SO_4] = 1.5 \times 10^8$ cm^{-3} (curves) and 4.3×10^7 cm^{-3} (straight lines); **b**, at 278 K and $[H_2SO_4] = 6.3 \times 10^7$ cm^{-3}. All measurements were made at 38% relative humidity. Triangles, J_{ch}; filled circles, J_{gcr}; open circles, J_n. The fitted lines are drawn to guide the eye. The bars indicate 1σ total errors, although the overall ammonia scale uncertainty of a factor 2 is not shown.

of sulphuric acid. Here 'pure' implies only H_2SO_4 and H_2O, although we point out that no water molecules were detected because they were lost by collisional dissociation or rapid evaporation from the sulphuric acid clusters on entering the vacuum of the instrument. At 292 K, pure acid clusters with $n \geq 4$ were highly suppressed, showing that the charged pure tetramer was unstable and evaporated rapidly. The clusters grew by a striking stepwise accretion of NH_3 molecules, each stabilizing a distinct additional number of acid molecules, depending on the ammonia concentration. Figure 3d shows how the cluster maintained a strict 1:1 molar ratio of ammonia and sulphuric acid as it grew, suggesting that the most stable growth path involved ammonium bisulphate ($NH_4^+HSO_4^-$) cluster formation. All clusters showed this 1:1 molar ratio above 100 p.p.t.v. ammonia—and a decreased NH_3 content below. The observed change in the nucleation rate from a strong to weak NH_3 dependence at some value below 100 p.p.t.v. (Fig. 4) is therefore explained as a transition from NH_3-limited to NH_3-saturated nucleation (that is, where each acid molecule condensing on the cluster is immediately stabilized by an ammonia molecule, thereby suppressing its evaporation). Quantum chemical calculations indicate that NH_3 and amines bind strongly to neutral acid clusters[31], indicating that ternary nucleation of neutral clusters above $n = 1$ may proceed by the same mechanism as that observed for charged clusters above $n = 4$, after which the negative charge becomes sufficiently shielded to allow NH_3 to bind. We term this stepwise stabilization of H_2SO_4 clusters the base-stabilization nucleation mechanism.

The CLOUD measurements address a long-standing controversy in atmospheric nucleation, namely whether binary nucleation of sulphuric acid and water vapour can account for new particle formation in the boundary layer. Figure 5 presents a comparison of our GCR nucleation rates with atmospheric observations of boundary-layer nucleation[8,32,33] and recent laboratory experiments[19,29]. We find that ion-induced binary nucleation proceeds at a significant rate in the cool temperatures of the free troposphere at atmospheric concentrations of sulphuric acid, and may be an important process when ternary vapour concentrations are low. Some fraction of these particles may be transported downwards and could constitute an important source in the remote marine boundary layer. In contrast, we show that binary

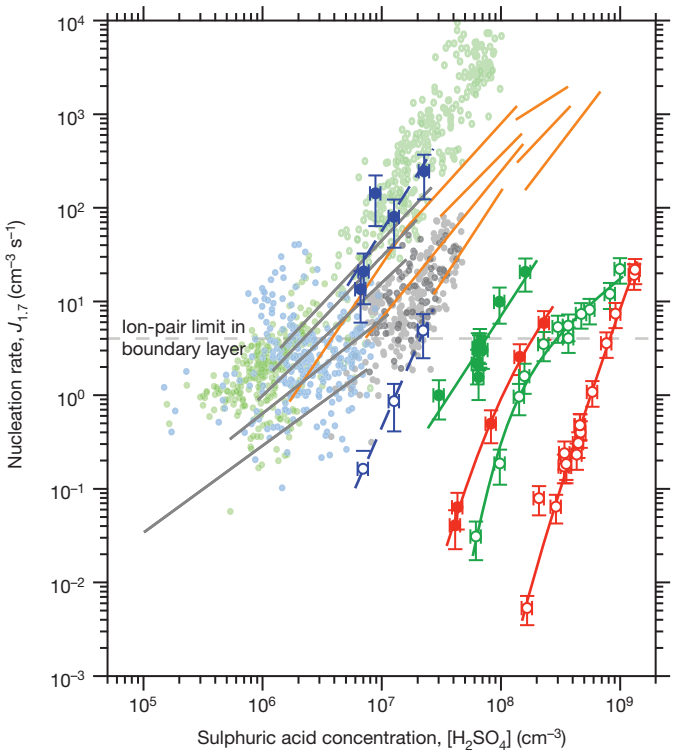

Figure 5 | Nucleation rate comparison. Comparison of CLOUD data with measurements of the nucleation rate of new particles as a function of [H_2SO_4] in the atmospheric boundary layer (pale filled circles[8,33] and pale open circles[32]) and with recent laboratory experiments at room temperature (grey[19] and orange[29] lines). The CLOUD data (large, darker symbols and lines) show the galactic cosmic ray nucleation rates, J_{gcr}, measured at 248 K (blue), 278 K (green) and 292 K (red) and at NH_3 mixing ratios of <35 p.p.t.v. (open green and red circles), <50 p.p.t.v. (open blue circles), 150 p.p.t.v. (filled blue and green circles) and 190 p.p.t.v. (filled red circles). The bars indicate 1σ total errors, although the overall factor 2 scale uncertainty on [H_2SO_4] is not shown. The measurements at 278 and 292 K bracket the typical range of boundary-layer temperatures, whereas those at 248 K reflect exceptionally cold conditions. Ion-induced nucleation in the boundary layer is limited by the ion-pair production rate to a maximum of about 4 cm^{-3} s^{-1}.

nucleation within the boundary layer is negligible in all except the coldest conditions, so additional species are required. It has been reported[29] that H_2SO_4 at atmospheric concentrations can explain atmospheric nucleation rates in most locations even without the clear participation of ammonia or organic substances. In view of the CLOUD results, we consider it likely that the result in ref. 29 was affected by the presence of ternary vapours below the detection limits of the experiment.

Under the conditions studied so far in CLOUD (no intentional addition of organic vapours), essentially all nucleating sulphuric acid clusters at 292 K include nitrogen-containing bases or amides: NH_3, amines or urea. However, for typical boundary-layer ammonia mixing ratios, below about 1 p.p.b.v., ternary nucleation of NH_3–H_2SO_4–H_2O, with or without ions, is unable to explain atmospheric observations (Figs 4 and 5). This implies that other species, most probably organic compounds[18,19], are necessary for boundary-layer nucleation.

The CLOUD experiment provides direct measurements of the molecular composition from single molecule to stable aerosol particle. This has provided new insight into how the ternary nucleation of sulphuric acid particles in the region of the critical cluster proceeds by a base-stabilization mechanism: the clusters grow by a stepwise accretion of basic molecules, each stabilizing a distinct additional number of acid molecules in the cluster, depending on the vapour concentrations.

The CLOUD measurements have also quantified the enhancement of ion-induced nucleation compared with neutral nucleation. Ground-level GCR ionization substantially increases the nucleation rate of sulphuric acid and sulphuric acid–ammonia particles, by between twofold and tenfold or more, provided that the nucleation rate lies below the limiting ion-pair production rate. Although we have not yet duplicated the concentrations or complexities of atmospheric organic vapours, we find that ion enhancement of nucleation occurs for all temperatures, humidities and cluster compositions observed so far. Ion-induced nucleation will manifest itself as a steady production of new particles that is difficult to isolate in atmospheric observations because of other sources of variability but is nevertheless taking place and could be quite large when averaged globally over the troposphere. However, the fraction of these freshly nucleated particles that grow to sufficient sizes to seed cloud droplets, as well as the role of organic vapours in the nucleation and growth processes, remain open questions experimentally. These are important findings for the potential link between galactic cosmic rays and clouds.

METHODS SUMMARY

CLOUD is designed to study the effects of cosmic rays on aerosols, cloud droplets and ice particles, under precisely controlled laboratory conditions. The CLOUD chamber and gas system have been built to the highest technical standards of cleanliness and performance. Owing to its large volume (26 m^3) and highly stable operating conditions, the chamber allows nucleation rates to be reliably measured over a wide range from 0.001 to well above 100 cm^{-3} s^{-1}. The loss rate of condensable vapours onto the walls of the chamber (0.0015 s^{-1}) is comparable to the condensation sink rate onto ambient aerosols under pristine atmospheric boundary-layer conditions. The experiment has several unique aspects, including precise control of the 'cosmic ray' beam intensity from the CERN Proton Synchrotron, the capability to create an ion-free environment with an internal electric clearing field, precise and uniform adjustment of the H_2SO_4 concentration by means of ultraviolet illumination from a fibre-optic system, and highly stable operation at any temperature between 300 and 183 K. The contents of the chamber are continuously analysed by a suite of instruments connected to sampling probes that project into the chamber.

Full Methods and any associated references are available in the online version of the paper at www.nature.com/nature.

Received 9 September 2010; accepted 24 June 2011.

1. IPCC. *Climate Change 2007: the Physical Science Basis. Contribution of Working Group I to the Fourth Assessment Report of the Intergovernmental Panel on Climate Change* (Cambridge Univ. Press, 2007).
2. Feingold, G. & Siebert, H. in *Clouds in the Perturbed Climate System* (eds Heintzenberg, J. & Charlson, R.J.) 319–338 (MIT Press, 2009).
3. Rosenfeld, D. *et al.* Flood or drought: how do aerosols affect precipitation? *Science* **321,** 1309–1313 (2008).
4. Merikanto, J., Spracklen, D. V., Mann, G. W., Pickering, S. J. & Carslaw, K. S. Impact of nucleation on global CCN. *Atmos. Chem. Phys.* **9,** 8601–8616 (2009).
5. Spracklen, D. V. *et al.* Contribution of particle formation to global cloud condensation nuclei concentrations. *Geophys. Res. Lett.* **35,** L06808, doi:10.1029/2007GL033038 (2008).
6. Pierce, J. R. & Adams, P. J. Can cosmic rays affect cloud condensation nuclei by altering new particle formation rates? *Geophys. Res. Lett.* **36,** L09820, doi:10.1029/2009GL037946 (2009).
7. Zhang, R. Getting to the critical nucleus of aerosol formation. *Science* **328,** 1366–1367 (2010).
8. Kerminen, V.-M. *et al.* Atmospheric nucleation: highlights of the EUCAARI project and future directions. *Atmos. Chem. Phys.* **10,** 10829–10848 (2010).
9. Boy, M. *et al.* Sulphuric acid closure and contribution to nucleation mode particle growth. *Atmos. Chem. Phys.* **5,** 863–878 (2005).
10. Wang, L. *et al.* Atmospheric nanoparticles formed from heterogeneous reactions of organics. *Nature Geosci.* **3,** 238–242 (2010).
11. Ziereis, H. & Arnold, F. Gaseous ammonia and ammonium ions in the free troposphere. *Nature* **321,** 503–505 (1986).
12. Coffman, D. J. & Hegg, D. A. A preliminary study of the effect of ammonia on particle nucleation in the marine boundary layer. *J. Geophys. Res.* **100** (D4), 7147–7160 (1995).
13. Ball, S. M., Hanson, D. R., Eisele, F. L. & McMurry, P. H. Laboratory studies of particle nucleation: initial results for H_2SO_4, H_2O, and NH_3 vapors. *J. Geophys. Res.* **104,** 23709–23718 (1999).
14. Zhang, R. *et al.* Atmospheric new particle formation enhanced by organic acids. *Science* **304,** 1487–1490 (2004).
15. Murphy, S. M. *et al.* Secondary aerosol formation from atmospheric reactions of aliphatic amines. *Atmos. Chem. Phys.* **7,** 2313–2337 (2007).
16. Berndt, T. *et al.* Laboratory study on new particle formation from the reaction OH + SO_2: influence of experimental conditions, H_2O vapour, NH_3 and the amine

tert-butylamine on the overall process. *Atmos. Chem. Phys.* **10,** 7101–7116 (2010).
17. Smith, J. N. *et al.* Observations of aminium salts in atmospheric nanoparticles and possible climatic implications. *Proc. Natl Acad. Sci. USA* **107,** 6634–6639 (2010).
18. Zhang, R. *et al.* Formation of nanoparticles of blue haze enhanced by anthropogenic pollution. *Proc. Natl Acad. Sci. USA* **106,** 17650–17654 (2009).
19. Metzger, A. *et al.* Evidence for the role of organics in aerosol particle formation under atmospheric conditions. *Proc. Natl Acad. Sci. USA* **107,** 6646–6651 (2010).
20. Arnold, F. Multi-ion complexes in the stratosphere—implications for trace gases and aerosol. *Nature* **284,** 610–611 (1980).
21. Raes, F., Janssens, A. & Van Dingenen, R. The role of ion-induced aerosol formation in the lower atmosphere. *J. Aerosol Sci.* **17,** 466–470 (1986).
22. Turco, R. P., Zhao, J.-X. & Yu, F. A new source of tropospheric aerosols: Ion–ion recombination. *Geophys. Res. Lett.* **25,** 635–638 (1998).
23. Lovejoy, E. R., Curtius, J. & Froyd, K. D. Atmospheric ion-induced nucleation of sulfuric acid and water. *J. Geophys. Res.* **109,** D08204, doi:10.1029/2003JD004460 (2004).
24. Sorokin, A. & Arnold, F. Laboratory study of cluster ions formation in H_2SO_4–H_2O system: implications for threshold concentration of gaseous H_2SO_4 and ion-induced nucleation kinetics. *Atmos. Environ.* **41,** 3740–3747 (2007).
25. Eichkorn, S., Wilhelm, S., Aufmhoff, H., Wohlfrom, K. H. & Arnold, F. Cosmic ray-induced aerosol-formation: first observational evidence from aircraft-based ion mass spectrometer measurements in the upper troposphere. *Geophys. Res. Lett.* **29,** 1698–1701 (2002).
26. Lee, S. H. *et al.* Particle formation by ion nucleation in the upper troposphere and lower stratosphere. *Science* **301,** 1886–1889 (2003).
27. Svensmark, H. & Friis-Christensen, E. Variation of cosmic ray flux and global cloud coverage—a missing link in solar-climate relationships. *J. Atmos. Sol. Terr. Phys.* **59,** 1225–1232 (1997).
28. Kirkby, J. Cosmic rays and climate. *Surv. Geophys.* **28,** 333–375 (2007).
29. Sipilä, M. *et al.* The role of sulfuric acid in atmospheric nucleation. *Science* **327,** 1243–1246 (2010).
30. Kazil, J. & Lovejoy, E. R. A semi-analytical method for calculating rates of new sulfate aerosol formation from the gas phase. *Atmos. Chem. Phys.* **7,** 3447–3459 (2007).
31. Kurtén, T., Loukonen, V., Vehkamäki, H. & Kulmala, M. Amines are likely to enhance neutral and ion-induced sulfuric acid–water nucleation in the atmosphere more effectively than ammonia. *Atmos. Chem. Phys.* **8,** 4095–4103 (2008).
32. Kuang, C., McMurry, P. H., McCormick, A. V. & Eisele, F. L. Dependence of nucleation rates on sulfuric acid vapor concentration in diverse atmospheric locations. *J. Geophys. Res.* **113,** D10209, doi:0.1029/2007JD009253 (2008).
33. Paasonen, P. *et al.* Connection between new particle formation and sulfuric acid at Hohenpeissenberg (Germany) including the influence of organic compounds. *Boreal Envir. Res.* **14,** 616–629 (2009).

Supplementary Information is linked to the online version of the paper at www.nature.com/nature.

Acknowledgements We thank CERN for supporting CLOUD with important technical and financial resources, and for providing a particle beam from the CERN Proton Synchrotron. We also thank J.-L. Agostini, S. Atieh, J. Baechler, D. Bloess, G. Bowden, A. Braem, T. Callamand, A. Castel, L.-P. De Menezes, G. Favre, L. Ferreira, L. Gatignon, D. Gregorio, M. Guinchard, E. Ivanova, F. Josa, I. Krasin, R. Kristic, A. Kuzmin, O. Maksumov, S. Mizin, R. Richter, R. Sitals, A. Vacca, R. Veenhof, A. Wasem and M. Wilhelmsson for their contributions to the experiment. This research has received funding from the EC Seventh Framework Programme under grant agreement no. 215072 (Marie Curie Initial Training Network, 'CLOUD-ITN') and ERC-Advanced Grant 'ATMNUCLE' no. 227463, the German Federal Ministry of Education and Research (project no. 01LK0902A), the Swiss National Science Foundation (project nos 206621_125025 and 206620_130527), the Academy of Finland Center of Excellence program (project no. 1118615), the Austrian Science Fund (FWF; project nos P19546 and L593), and the Russian Academy of Sciences and Russian Foundation for Basic Research (grant N08-02-91006-CERN).

Author Contributions J.A. performed the nucleation rate analysis. S.S. conducted the APi-TOF analysis. J.A., F.B., M.B., A. Downard, E.D., J. Duplissy, S.E., A.F., S.G., D.H., L.I., W.J., J.K., F.K., A. Kürten, A. Kupc, K.L., V.M., A.M., T.N., F.R., L.R., R.S., S.S., Y.S., G.T. and D.W. conducted the data collection and analysis. J.A., K.S.C., J.C., E.D., S.E., L.I., E.R.L. and F.S. performed the modelling. J.K. wrote the manuscript. U.B., K.S.C., J.C., J.K., M.K., J.H.S. and D.R.W. did data interpretation and editing of the manuscript. All authors contributed to the development of the CLOUD facility and analysis instruments, and commented on the manuscript.

Author Information Reprints and permissions information is available at www.nature.com/reprints. The authors declare no competing financial interests. Readers are welcome to comment on the online version of this article at www.nature.com/nature. Correspondence and requests for materials should be addressed to J.K. (jasper.kirkby@cern.ch).

METHODS

The CLOUD chamber (Supplementary Fig. 1) is a 3-m-diameter electropolished stainless steel cylinder of 26.1 m^3. After tests with a pilot experiment[34], the chamber and gas supply are designed to achieve the highest standards of cleanliness and temperature stability. To stimulate photolytic reactions—in particular the oxidation of SO_2 to H_2SO_4 in the presence of O_3 and H_2O—the contents of the chamber are irradiated by ultraviolet radiation in the range 250–400 nm, introduced by means of 250 optical fibre vacuum feedthroughs installed on top of the chamber. The chamber temperature is controlled by precisely regulating the temperature of the air circulating in the space between the chamber and its surrounding thermal housing. Experiments can be performed at temperatures between 300 and 183 K. In addition, the chamber can be raised to 373 K for bakeout cleaning. The temperature stability of the chamber is about ± 0.01 K, with no observable change when the ultraviolet lights are turned on at full power. The nominal operating pressure is one atmosphere. However, rapid adiabatic expansions of up to 200 mbar can be generated to operate in a classical cloud chamber mode for the creation and growth of droplets and ice particles.

Pure air, free of condensable vapours, is obtained from the evaporation of cryogenic liquid N_2 and liquid O_2, mixed in the ratio 79:21, respectively. The air is humidified with a Nafion humidifier using water stabilized to ± 0.01 K and purified by recirculation through a bank of Millipore Super-Q filters and irradiated with ultraviolet radiation to suppress biological activity. Ozone is added to the inlet air by ultraviolet irradiation (less than 200 nm). Trace gases such as SO_2 or NH_3 are obtained from gas cylinders containing 100 p.p.m.v. and 1% concentrations, respectively, in pressurized N_2. Each trace gas is diluted with pure air to the required concentration before entering the chamber, and has an individual circuit, with an isolation valve at the chamber, to avoid cross-contamination or reactions with other gases outside the chamber. To suppress contamination from plastic materials, the gas piping is made from stainless steel, and all chamber seals and most gas seals are metal (gold-coated to render them chemically inert). To compensate for sampling losses, there is a continuous flow of fresh gases into the chamber of 85 l min^{-1}, resulting in a dilution lifetime of 5 h.

The chamber can be exposed to a 3.5 GeV/c secondary π^+ beam from the CERN Proton Synchrotron, spanning the galactic cosmic-ray intensity range from ground level to the stratosphere. The beam is defocused to a transverse size of about 1.5×1.5 m^2 at the chamber. The horizontal and vertical beam profiles and rates are measured with a plastic scintillator hodoscope. An ionization-counter array, located nearby but outside the beam region, monitors the ambient flux and angular distribution of galactic cosmic rays. Two stainless steel fans are mounted inside the chamber, and coupled magnetically to flexible drives connected to motors located outside the thermal housing. The fans produce a counter-flow inside the chamber, to rapidly mix the fresh gases and the ions generated by the pion beam, and ensure good uniformity. To study neutral nucleation, the beam is turned off and an internal electric field of up to 20 kV m^{-1} is applied by means of two transparent field cage electrodes. This rapidly (in about 1 s) sweeps out the background ions produced by galactic cosmic rays. The electrodes are supported on partly conducting ceramic insulators to eliminate surface charges and stray electric fields when the high voltage is set to zero.

The contents of the chamber are continuously analysed by instruments connected to sampling probes that project 0.5 m into the chamber. The chamber instrumentation for the results reported here comprise a chemical ionization mass spectrometer (CIMS) for H_2SO_4 concentration, an atmospheric pressure interface time-of-flight (APi-TOF) mass spectrometer for molecular composition of positive and negative ions up to 2,000 Th (thomson units; 1 Th = 1 Da/e)[35], a condensation particle counter (CPC) battery at 2.5–12-nm thresholds (mobility diameters), a di-ethylene glycol CPC (DEG-CPC) at 2.0 nm threshold[36], a scanning particle size magnifier (PSM) in the threshold range 1.3–2 nm[37], a radial differential mobility analyser (rDMA) in the size range 2–10 nm[38], a scanning mobility particle sizer (SMPS) in the size range about 10–100 nm, a neutral cluster and air ion spectrometer (NAIS)[39], a small-ion counter (Gerdien counter), trace gas analysers (O_3 and SO_2), a proton transfer reaction time-of-flight (PTR-TOF) mass spectrometer for organic vapour concentrations[40], two instruments for NH_3 measurements (a long-path absorption photometer (LOPAP) and a proton transfer reaction mass spectrometer (PTR-MS)[41]), and instruments to measure chamber conditions (dewpoint, ultraviolet intensity, temperature and pressure). A central data acquisition (DAQ) system controls the operating conditions of the experiment, collects and backs up the data from the instruments, provides multi-user access for monitoring the performance of the instruments and chamber, and provides real-time physics analysis using the combined data from multiple instruments.

The APi-TOF[35] measures the ion cluster mass spectra in the chamber. Chemical species are identified from their exact mass signatures and isotopic fractions. Owing to the high mass resolution ($\Delta m/m = 3 \times 10^{-4}$) and accuracy ($\delta m/m < 2 \times 10^{-5}$) of this instrument, unambiguous identification of the constituent chemical species is achieved for almost all charged clusters up to a mass/charge limit of 2,000 Th. This excludes water molecules, which are lost by collisional dissociation or rapid evaporation from the sulphuric acid clusters on entering the vacuum of the instrument. Previous measurements have established that water molecules are indeed present in these charged clusters[42]. In contrast, the evaporation of ammonia and amine molecules from acid clusters in the APi-TOF is thought to be small. This is supported by the sharp cluster maxima seen in Fig. 3d.

Examples of raw APi-TOF spectra during nucleation events without additional NH_3 at 292 K are shown in Supplementary Fig. 3. The negative-ion spectrum shows strong peaks corresponding to the charged monomer, dimer and trimer of sulphuric acid (A_n^-, n = 1–3, where A represents H_2SO_4 or the HSO_4^- ion); higher sulphuric acid clusters ($n > 3$) are predominantly accompanied by an additional species that is either NH_3, dimethylamine or ethylamine. In contrast, the positive-ion spectrum shows no evidence for any sulphuric acid molecules, but shows pure water clusters, $H_3O^+(H_2O)_n$, $n \leq 3$, and a broad range of organic compounds, of which strong lines are usually produced by protonated pyridine ($C_5H_5N.H^+$), urea ($CH_4N_2O.H^+$), dimethylamine and ethylamine ($C_2H_7N.H^+$), and $C_3H_8N_2O.H^+$, which corresponds to dimethylurea or other compounds (mostly amides).

The nucleation rates are obtained from the formation rates, dN_d/dt (where the subscript d refers to the detection threshold diameter of the particle counter), measured with a TSI 3776 CPC (50% detection threshold diameter $d = 2.5$ nm), DEG-CPC (2.0 nm) and PSM (1.7, 1.9 and 2.1 nm)[43,44]. The nucleation rates are determined at the critical size (taken to be 1,200 Da, or about 1.7 nm mobility diameter) from measurements made with particle counters at thresholds between 2 and 2.5 nm, because the PSM was not available for the entire campaign. To determine the nucleation rates, the measured formation rates are corrected for losses between 1.7 nm and the detection size threshold. This requires experimental measurements of the wall loss rates and particle growth rates. Other losses, such as coagulation and dilution losses are also accounted for, but are negligible. The corrections are calculated with a kinetic model (AeroCLOUD) and are cross-checked analytically[43,44]. The nucleation rates are independently verified by direct measurements with the PSM at 1.7 nm threshold, where available.

Neutral nucleation rates are measured with zero beam and with the field cage electrodes set to ± 30 kV. This completely suppresses ion-induced nucleation because, under these conditions, small ions are swept from the chamber in about 1 s. For ion-induced nucleation to produce a critical cluster that is not removed by the electric field, the primary negative ion from a traversing ionizing particle must, within 1 s, reach an H_2SO_4 molecule, which grows beyond the critical size and is then neutralized by ion–ion recombination before reaching an electrode or the chamber wall. In the presence of the electric field, the recombination lifetime alone is estimated to exceed 5×10^4 s, so ion-induced nucleation can be completely excluded as a background to the measured neutral nucleation rates.

The error on J has three components, which are added together in quadrature to provide the total error indicated in Fig. 1: first, a statistical measurement error derived from the scatter of the particle counter measurements, evaluated separately for each nucleation event; second, an estimated $\pm 50\%$ uncertainty on the modelled correction factor, $J_{1.7}/J_d$, where J_d is the nucleation rate at size d, obtained after correcting dN_d/dt for detection losses, and third, an estimated $\pm 30\%$ systematic uncertainty on J_d estimated from the run-to-run reproducibility of dN_d/dt under nominally identical chamber conditions.

When the chamber is operated below 292 K, the particle counters and certain other detectors are cooled to about 280 K to minimize cluster evaporation on entering the warm instrument from a cold chamber and sampling probe. However, we caution that the measurements presented here at low temperatures are subject to uncorrected evaporation effects due to relatively warm instruments.

The overall experimental uncertainty on $[H_2SO_4]$ measured by the CIMS is estimated to be $-50\%/+100\%$, on the basis of three independent measurements: particle growth rate, the depletion rate of $[SO_2]$ by photo-oxidation, and an external calibration source. However, the run-to-run relative experimental uncertainty on $[H_2SO_4]$ is smaller, typically $\pm 10\%$. The concentrations of SO_2, O_3 are measured with calibrated instruments and are known to $\pm 10\%$. The overall uncertainty on the NH_3 mixing ratio is estimated to be $-50\%/+100\%$. Ammonia mixing ratios are measured with a PTR-MS and LOPAP. Although the former is more sensitive (5 p.p.t.v. lower detection limit compared with 35 p.p.t.v. for the LOPAP), the sampling probe of the LOPAP has a higher efficiency, resulting in a higher overall sensitivity for the LOPAP. Because liquid water

is used in its sampling probe, the LOPAP only provides measurements above 273 K.

34. Duplissy, J. *et al.* Results from the CERN pilot CLOUD experiment. *Atmos. Chem. Phys.* **10,** 1635–1647 (2010).
35. Junninen, H. *et al.* A high-resolution mass spectrometer to measure atmospheric ion composition. *Atmos. Meas. Tech.* **3,** 1039–1053 (2010).
36. Iida, K., Stolzenburg, M. R. & McMurry, P. H. Effect of working fluid on sub-2 nm particle detection with a laminar flow ultrafine condensation particle counter. *Aerosol Sci. Technol.* **43,** 81–96 (2009).
37. Vanhanen, J. *et al.* Particle size magnifier for nano-CN detection. *Aerosol Sci. Technol.* **45,** 533–542 (2011).
38. Brunelli, N. A., Flagan, R. C. & Giapis, K. P. Radial differential mobility analyzer for one nanometer particle classification. *Aerosol Sci. Technol.* **43,** 53–59 (2009).
39. Kulmala, M. *et al.* Towards direct measurement of atmospheric nucleation. *Science* **318,** 89–92 (2007).
40. Graus, M., Müller, M. & Hansel, A. High resolution PTR-TOF: quantification and formula confirmation of VOC in real time. *J. Am. Soc. Mass Spectrom.* **21,** 1037–1044 (2010).
41. Norman, M., Hansel, A. & Wisthaler, A. O_2^+ as reagent ion in the PTR-MS instrument: detection of gas-phase ammonia. *Int. J. Mass Spectrom.* **265,** 382–387 (2007).
42. Froyd, K. D. & Lovejoy, E. R. Experimental thermodynamics of cluster ions composed of H_2SO_4 and H_2O. 2. Measurements and *ab initio* structures of negative ions. *J. Phys. Chem. A* **107,** 9812–9824 (2003).
43. Kerminen, V.-M. & Kulmala, M. Analytical formulae connecting the 'real' and the 'apparent' nucleation rate and the nuclei number concentration for atmospheric nucleation events. *J. Aerosol Sci.* **33,** 609–622 (2002).
44. Kulmala, M. & Kerminen, V.-M. On the formation and growth of atmospheric nanoparticles. *Atmos. Res.* **90,** 132–150 (2008).